Preprints, Joint 8th IFAC Symposium on System Structure and Control,
17th IFAC Workshop on Time Delay Systems, 5th IFAC Workshop on
Linear Parameter Varying Systems. Montreal, Canada, September 27-30, 2022

Time-domain simulation and testing for dynamic force and stability prediction in milling: Collaboration with feed rate scheduling software

Tony Schmitz*. Jose Nazario* Timothy No* Michael Gomez Greg Corson***

* *University of Tennessee, Knoxville, Knoxville, TN 37966, USA (Tel: 865-974-6141; e-mail: tony.schmitz@utk.edu; e-mail: jnazari1@utk.edu; e-mail: tno@vols.utk.edu; e-mail: gcorson@vols.utk.edu).*

** *MSC Industrial Supply Co., Knoxville, TN 37932, USA (e-mail: michael.gomez@mscdirect.com)*

Abstract: This paper describes: 1) the use of feed rate scheduling software to predict the radial depth of cut variation for three-axis milling toolpaths and; 2) the use of this radial depth profile in a time-domain simulation to predict dynamic cutting forces. The time-domain simulation, which also includes the tool tip frequency response functions and force model (which relates the cutting force components to the chip geometry) as inputs, enables dynamic force profiles to be predicted and parameter combinations that cause chatter to be identified. A ramp geometry is selected that provides constantly varying radial depth and force predictions are completed at multiple axial depths for comparison to measured forces.

Keywords: Milling; dynamics; chatter; simulation

1. INTRODUCTION

Predictive models are required to select optimal milling parameters, including axial and radial depths of cut, spindle speed, and feed per tooth, at the process planning stage. The intent is to select parameters that enable first part correct performance to avoid costly and time-consuming trial and error parameter identification. This first part correct performance requires that chatter, or self-excited vibration, does not occur and acceptable geometric accuracy and surface finish are achieved. Available predictive models for milling dynamics include: analytical, frequency-domain solutions for milling stability from Altintas and Budak (1995) and surface location error (SLE, forced vibration which leads to part geometry errors) by Schmitz and Mann (2006); time-domain simulation for milling force and vibration, which can be used to assess stability and SLE from Schmitz and Smith (2009); and semi-discretization methods for milling force and vibration, which can again be used to assess stability and SLE by Insperger et al. (2006). The purpose of these models is to relate the milling parameters, process dynamics, and milling performance in a mathematical framework.

Another class of predictive models relates the milling parameters to the cutting and non-cutting times given the part geometry. These computer-aided manufacturing (CAM) models use the peak cutting force, which depends on the part geometry, computer numerically controlled (CNC) tool path, and milling parameters, to modify the cutting and non-cutting times by updating the instantaneous feed rate along the tool path. The outcome is optimized cutting and non-cutting times for maximum productivity. This feed rate scheduling approach simultaneously consider the acceleration (and potentially jerk) limits of the CNC machining center drives from Dong et al. (2007) and Altintas and Erkorkmaz (2003), spline tool paths by Altintas and Erkorkmaz (2003), and cutting force by Yazar et al. (1994). Commercial feed rate scheduling software is gaining acceptance in industrial applications to optimize CNC part programs.

To date, however, these two predictive capabilities have remained separate. Machining dynamics models do not typically include the time-dependent cutting conditions imposed by CNC tool paths. They tend to focus on, for example, a fixed radial depth to determine stable combinations of spindle speed and axial depth in the graphical form of a stability map or the variation in SLE with spindle speed for a selected combination of radial depth, axial depth, and feed per tooth; both cases depend on the selected workpiece material. Feed rate scheduling solutions, on the other hand, do consider the variable cutting conditions for arbitrary three-axis and five-axis tool paths, but do not include the effects of relative vibration between the cutting tool and workpiece on the process stability and SLE. This relative vibration occurs because the tool and workpiece are not rigid and a complete solution requires more than geometry.

The purpose of this paper is to, for the first time, combine time-domain milling simulation and feed rate scheduling software to predict the dynamic cutting force components for a tool path with variable radial depth of cut. Both stable and unstable milling conditions are considered. The time-domain simulation inputs include the tool tip frequency response function (FRF, which describes the vibration behavior), cutting force model, and instantaneous radial depth of cut. The latter is obtained from the feed rate scheduling software Production Module provided by Third Wave Systems.

2. TIME-DOMAIN SIMULATION

Time-domain simulation provides numerical solution of the coupled, second-order, time-delay differential equations of

motion for milling in small time steps; see Schmitz and Smith (2009). It is well suited to incorporating the inherent complexities of milling dynamics, including tool geometries and the nonlinearity that occurs if the tooth leaves the cut due to large amplitude vibrations. The time-domain simulation used in this study predicts the time-dependent cutting force and vibration behavior by the following steps:

1. The instantaneous chip thickness, $h(t)$, is determined using the commanded chip thickness, instantaneous radial depth of cut, which depends on the CNC tool path, runout of the cutter teeth, and vibration of the current and previous teeth at the selected tooth angle for the current axial slice (discretized axial depth).
2. The cutting force components in the tangential, t, and normal, n, directions are calculated at each axial slice using the cutting force coefficients and process damping coefficients:

$$F_t(t) = k_{tc} b h(t) + k_{te} b - C_t \frac{b}{V} \dot{n} \quad (1)$$

$$F_n(t) = k_{nc} b h(t) + k_{ne} b - C_n \frac{b}{V} \dot{n} \quad (2)$$

where b is the axial slice width; the cutting force coefficients are identified by the subscripts t or n for direction and c or e for cutting or edge; the process damping coefficients are identified by the subscripts t or n for direction; V is the cutting speed; and $\dot{n}$ is the instantaneous tool vibration velocity in the normal (radial) direction. These forces are then summed over all axial slices engaged in the cut for the instantaneous radial depth.

3. The summed force components are used to find the new displacements by numerical (modified Euler) integration of the second-order delay differential equations of motion in the x (feed) and y directions:

$$m_x \ddot{x} + c_x \dot{x} + k_x x = F_t(t)\cos\phi + F_n(t)\sin\phi \quad (3)$$

$$m_y \ddot{y} + c_y \dot{y} + k_y y = F_t(t)\sin\phi - F_n(t)\cos\phi \quad (4)$$

where m is the tool tip modal mass, c is the modal viscous damping coefficient, k is the modal stiffness, and ϕ is the tool rotation angle; see Fig. 1. The subscripts (x or y) identify the direction. While these equations include only a single degree of freedom in each direction, multiple degrees-of-freedom in each direction can be accommodated by summing the modal contributions individually.

4. The tool rotation angle is incremented, and the process is repeated.

3. DATA COLLECTION

3.1 Force model

The four cutting force coefficients in (1) and (2) were identified experimentally using the average force, linear regression approach; see Schmitz and Smith (2009). Down milling tests were completed for: 3.18 mm radial depth (25% radial immersion), 9.0 mm axial depth, 7000 rpm spindle speed, and four feed per tooth values {0.03, 0.05, 0.07, 0.10} mm with the 6061-T6 extruded aluminum bar stock workpiece mounted on a Kistler 9257B cutting force dynamometer. The mean force in the x (feed) and y directions was plotted versus the commanded feed per tooth values and a linear regression was completed to identify the slope and intercept values. These slope and intercept values were then used to calculate the cutting force coefficients.

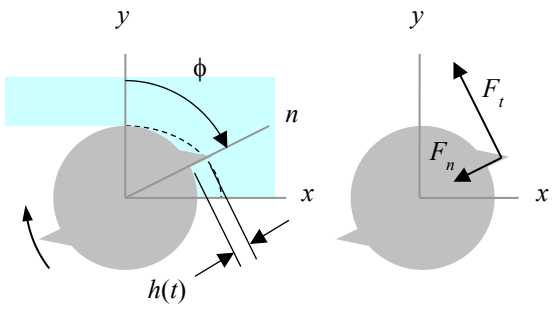

Figure 1. Milling model (up milling is shown, but the model is generic to up or down milling).

Table 1. Force model coefficient values.

Coefficient	Value	Units
k_{tc}	867×10^6	N/m^2
k_{nc}	332×10^6	N/m^2
k_{te}	6.7×10^3	N/m
k_{ne}	7.8×10^3	N/m
C_t	1.4×10^5	N/m
C_n	1.4×10^5	N/m

Process damping is described as energy dissipation due to interference between the cutting tool clearance face and machined surface during relative vibrations between the tool and workpiece; see work by Lee et al. (1995), Budak and Tunc (2010), and Tyler and Schmitz (2013). Tyler and Schmitz (2013) performed cutting tests to determine process damping coefficients for various workpiece materials. These results were used for this study, where the tangential and normal direction coefficients were assumed to be identical. The cutting force coefficients and process damping coefficients are listed in Table 1.

3.2 Tool tip FRFs

The tool tip FRF was measured by tap testing, where an instrumented hammer is used to excite the tool tip with a known force and the corresponding vibration response is measured using a low-mass accelerometer. These time responses are converted to the frequency domain using the Fourier transform and the ratio of the response to the force is calculated. The measurement was performed in both the x and y directions. The PCB Piezotronics hammer was model number 086C04 and the accelerometer was model number 352C23. The 12.7 mm diameter, four helical flute, square carbide endmill was produced by HTC and the model number

was 1.001-.500-1.375. A Maritool ER 32 collet holder (model number ER32-2.35) was used to clamp the tool and the spindle interface was CAT 40 for the Haas VF-4 three-axis CNC milling machine. A modal fit was performed for each FRF so the associated modal mass, damping coefficient, and stiffness values could be used in the simulation; see Table 2.

Table 2. Modal parameters from fits to measured tool tip FRFs.

m (kg)	k (N/m)	c (N-s/m)
	x direction	
123	1.37×10^{8}	1.24×10^{4}
3.47	1.34×10^{8}	2.67×10^{3}
0.70	5.96×10^{7}	4.07×10^{2}
0.22	9.55×10^{7}	4.52×10^{2}
0.19	1.37×10^{8}	3.46×10^{2}
0.07	6.83×10^{7}	2.33×10^{2}
0.04	5.26×10^{7}	1.25×10^{2}
0.11	2.00×10^{8}	5.35×10^{2}
1.25	2.30×10^{8}	2.00×10^{3}
20.8	1.47×10^{8}	9.39×10^{3}
	y direction	
3.19	1.19×10^{8}	1.83×10^{3}
1.48	9.57×10^{7}	1.14×10^{3}
2.45	2.32×10^{8}	1.83×10^{3}
1.99	2.42×10^{8}	1.69×10^{3}
1.32	2.43×10^{8}	2.08×10^{3}
0.29	1.23×10^{8}	3.95×10^{2}
0.20	1.50×10^{8}	4.38×10^{2}
0.09	8.71×10^{7}	2.46×10^{2}
0.04	5.27×10^{7}	1.30×10^{2}
0.09	1.57×10^{8}	5.71×10^{2}

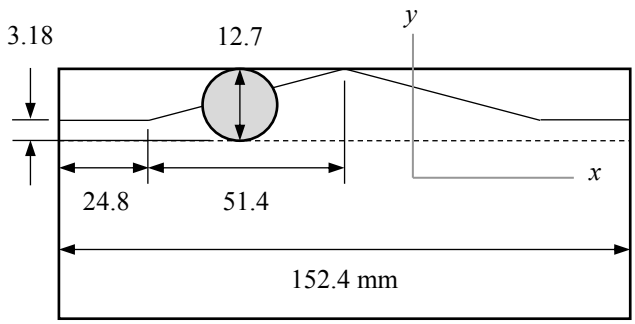

Figure 2. Part geometry. The ramp geometry continuously varied the radial depth from 3.18 mm (25% radial immersion) to 12.7 mm (slotting) and back for the left to right down milling operation. The axial depth (into the page) was constant and was varied between tests. The 12.7 mm diameter endmill is represented by the circle.

4. PART GEOMETRY

To provide a continuously variable radial depth of cut with a fixed axial depth, the part geometry displayed in Fig. 2 was selected. The combination of varying radial depth with fixed axial depth mimics traditional three-axis, 2.5D CNC machining toolpaths, where the material is removed with x-y planar toolpaths that implement the user-selected stepover (radial depth) and advance the stepdown in the z direction (axial depth) between each planar toolpath. The Fig. 2 geometry was machined multiple times using a different (constant) axial depth between tests to advance from stable (low axial depth) to unstable, or chatter, (high axial depth) cutting conditions. The workpiece material was 6061-T6 aluminum in all cases.

5. FEED RATE SCHEDULING SOFTWARE OUTPUT

Given the CAM toolpath and machining parameters, Production Module calculates the position-dependent radial depth of cut, angle of engagement between the rotating endmill and workpiece, and peak force values. For the part geometry shown in Fig. 2, the variation in radial depth of cut with cutting time is displayed in the top panel of Fig. 3. The constant radial depth of 3.18 mm is observed at the beginning and end of the toolpath. The radial depth increases from 3.18 mm (25% radial immersion) to 12.7 mm (slotting) at the center of the cut. The variation in angle of engagement is shown in the bottom panel of Fig. 3. The angle is 60 deg for the 25% radial immersion portion of the toolpath and increases to 180 deg for the slotting condition in the middle of the toolpath. For comparison, the angle of engagement calculated by both Production Module (PM) and time-domain simulation (TDS) are displayed.

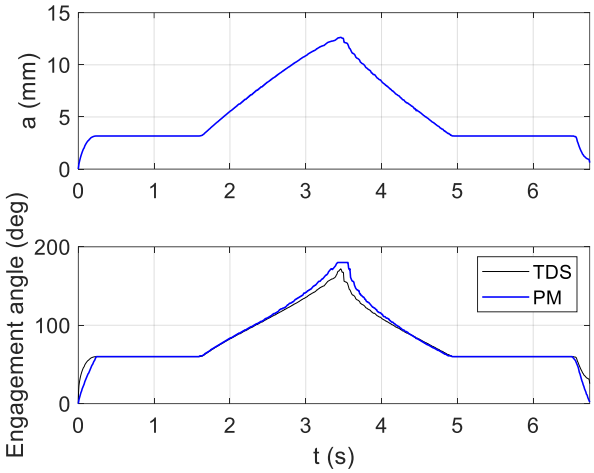

Figure 3. (Top) Variation in instantaneous radial depth of cut, a, with time for the part geometry shown in Fig. 5. (Bottom) Variation in engagement angle (i.e., tooth entry to exit angle for the down milling operation) with time.

The variation in radial depth/angle of engagement seen in Fig. 3 can cause the milling performance to transition from stable to unstable (chatter) behavior. This dependence of the milling performance on the axial/radial depth of cut, machining parameters, structural dynamics, and workpiece material motivates the combination of the feed rate scheduling software and time-domain simulation.

6. CUTTING FORCE MEASUREMENTS AND PREDICTIONS

Force measurements and predictions were completed for two workpiece geometries. First, the radial depth of cut was held constant and the measurement/prediction comparison was performed for variation axial depth-radial depth combinations to confirm the accuracy of the force model; see (1) and (2) with Table 1 coefficients. Second, the ramp profile was machined at multiple axial depths of cut and the measurement/prediction comparison was completed. For both geometries, the programmed toolpath was opened using Production Module and the radial depth of cut profile was predicted. This variation in radial depth with time in the toolpath served as a key input to the time-domain simulation. The peak force profiles were

also predicted by Production Module and compared to the measurement and time-domain simulation forces.

6.1 Constant radial depth

The setup described in Section 3.1 was used to machine a 6061-T6 aluminum workpiece bolted to a Kistler 9257B cutting force dynamometer. The radial depths of cut varied from 3.18 mm (25% radial immersion) to 12.7 mm (100% radial immersion) and the axial depths were varied from 3 mm to 12 mm. The spindle speed was 7000 rpm and the feed per tooth was 0.05 mm in all cases. Flood coolant was applied.

The first test case is for a 25% radial immersion down milling operation. The radial depth is 3.18 mm except at the cut entry and exit, where it increases and decreases with time. The axial depth for this case is 5 mm. The radial depth variation from Production Module was input to the time-domain simulation, as well as the tool tip FRFs and force model, and the simulation was used to predict the dynamic cutting force. Figure 4 shows the time-dependent resultant force, Fig. 5 shows the force variation during the cut entry (first 0.1 s), and Fig. 6 gives the steady-state force (1.4 s to 1.5 s). In all cases, the measured force was inverse filtered to remove the effects of the dynamometer dynamics.

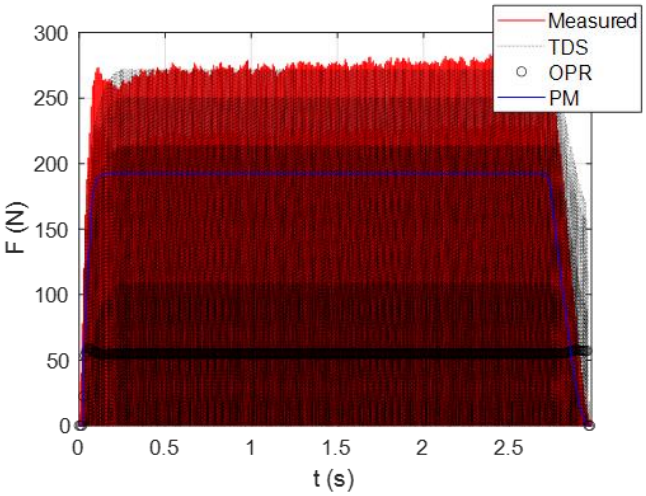

Figure 4. Resultant force for the constant 3.18 mm radial depth profile. The axial depth is 5 mm.

Figures 4-6 also include the once-per-revolution (OPR) samples from the time-domain simulation. These samples serve as a stability metric; see Honeycutt and Schmitz (2016). If the samples repeat during constant depth machining, this indicates forced vibration and stable cutting conditions. If they do not repeat during constant depth machining, this identifies self-excited vibration, or chatter. During variable radial depth machining, the transient nature of the signal means the OPR samples do not repeat. Stable cutting conditions are identified by the repeating OPR samples (circles) in Figs. 4-6. The variation in force amplitude from one tooth to the next in Figs. 5-6 is due to runout of the four teeth on the rotating endmill. The runout was measured using a dial indicator and included in the time-domain simulation.

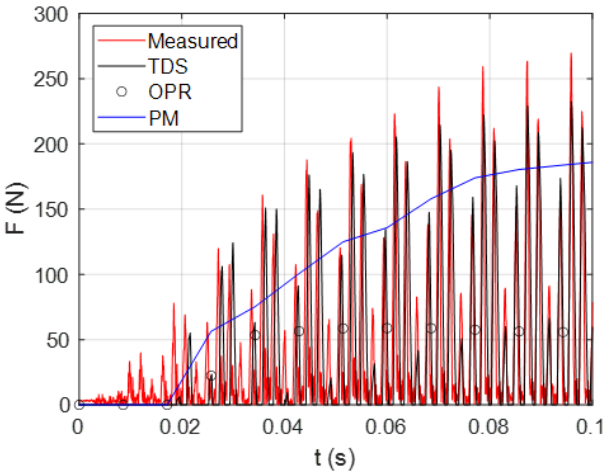

Figure 5. Transient resultant force for the cut entry from Fig. 7 (i.e., the first 0.1 s in Fig. 10). The axial depth is 5 mm.

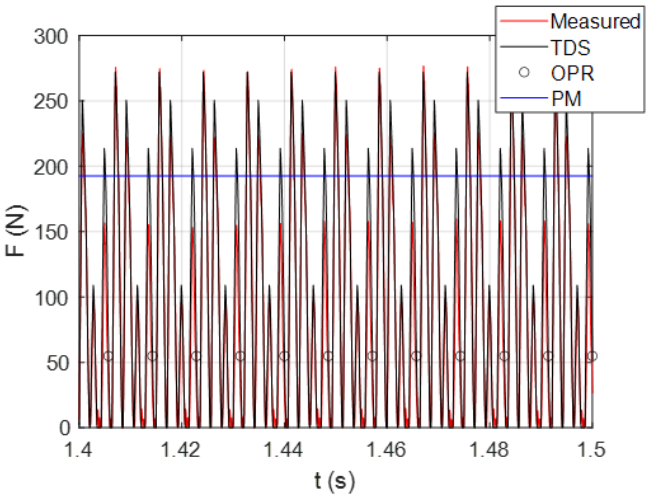

Figure 6. Steady-state resultant force from Fig. 7 (i.e., 0.1 s starting at 1.4 s in Fig. 10). The axial depth is 5 mm.

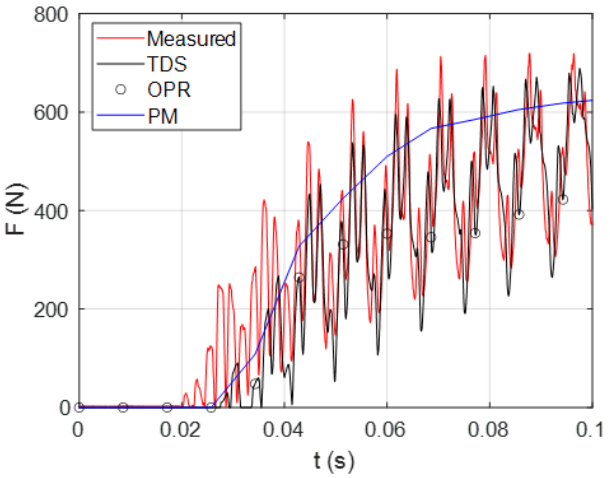

Figure 7. Transient resultant force for radial depth of 12.7 mm and axial depth of 12 mm.

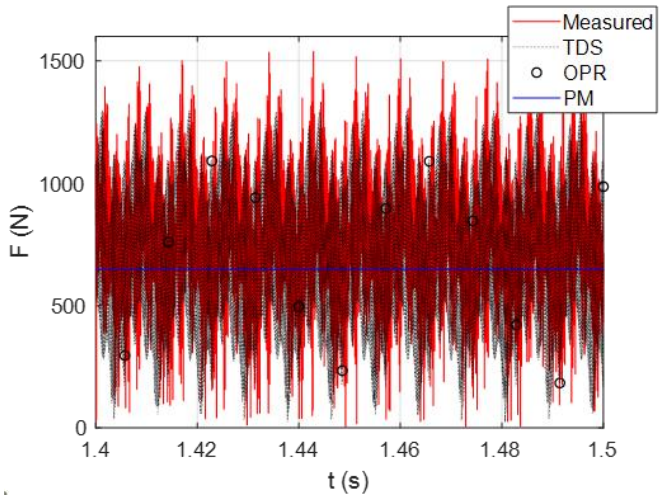

Figure 8. Steady-state resultant force for radial depth of 12.7 mm and axial depth of 12 mm.

The second constant radial depth of cut test case was performed with a radial depth of 12.7 mm (100% radial immersion) and axial depth of 12 mm; see Figs. 7 and 8. The selected depth of cut-spindle speed combination is unstable (chatter); this is demonstrated by the non-repeating OPR samples in Fig. 8. Note the large forces for the chatter conditions. The good agreement between the measured and time-domain simulation results validates the force model.

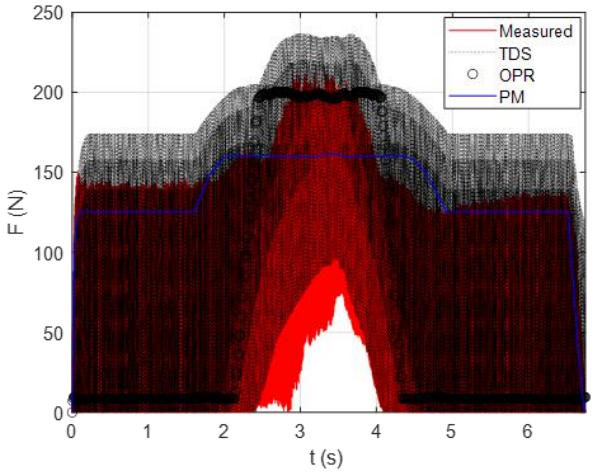

Figure 9. Resultant force for the ramp profile (radial depth described by Fig. 2). The axial depth is 7 mm.

6.2 Variable radial depth

The ramp profile's radial depth variation (from Production Module) was input to the time-domain simulation, as well as the tool tip FRFs and force model, and the dynamic cutting force was calculated for an axial depth of 7 mm. Fig. 9 displays the resultant force, Fig. 10 shows the force variation during the cut entry, and Fig. 11 gives the force near the middle of the toolpath. Note that this force is nominally constant because the cutting force is constant for a four-tooth endmill under slotting conditions with no runout; see Schmitz and Smith (2009). The repeated OPR samples in Fig. 11 show that the cut is stable and the TDS and measurement results agree.

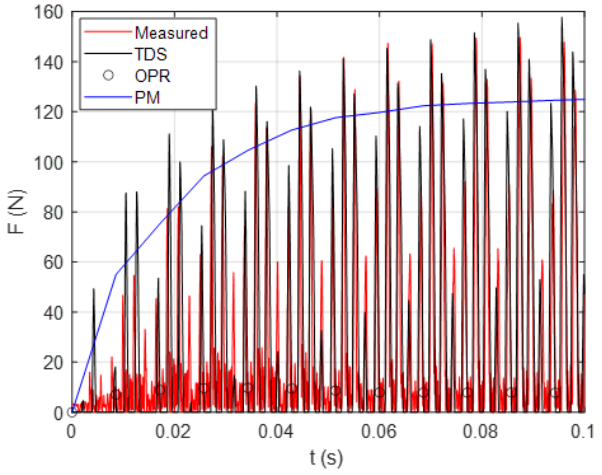

Figure 10. Transient resultant force for ramp profile with an axial depth of 7 mm.

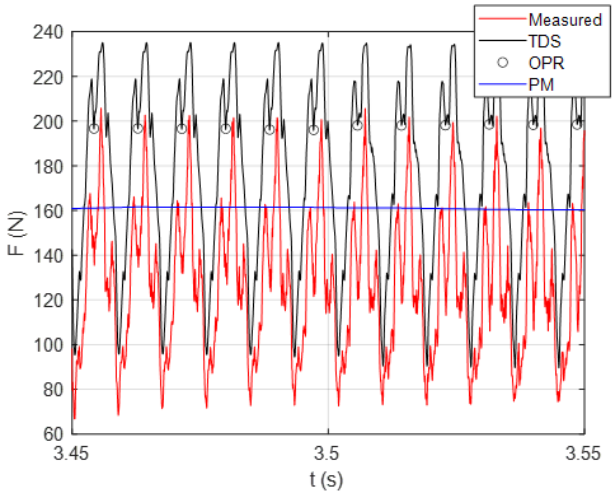

Figure 11. Resultant force for the ramp profile near center of toolpath. The axial depth is 7 mm.

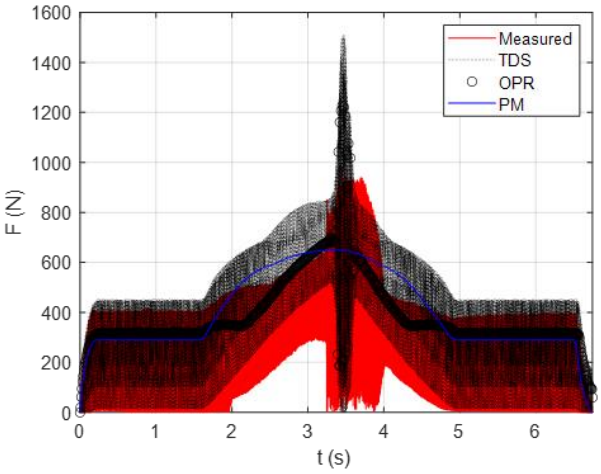

Figure 12. Resultant force for the ramp profile (radial depth described by Fig. 2). The axial depth is 12 mm.

Figures 12-14 display results for the second ramp case. The axial depth is 12 mm and the cutting conditions are now unstable near the middle of the toolpath. It is observed that

both the measured and TDS forces grow dramatically as the radial depth approaches 12.7 mm (slotting) and chatter occurs.

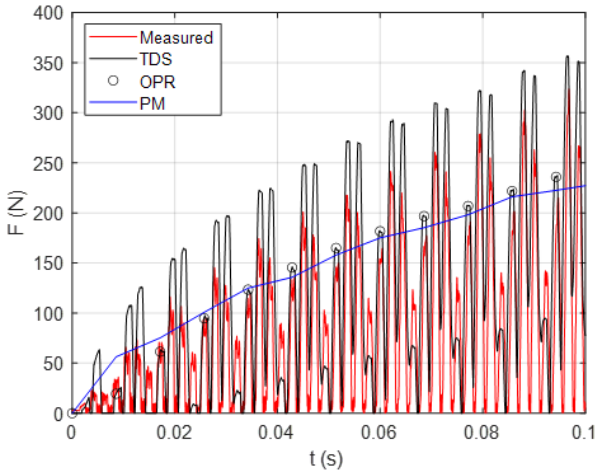

Figure 13. Transient resultant force for ramp profile with an axial depth of 12 mm.

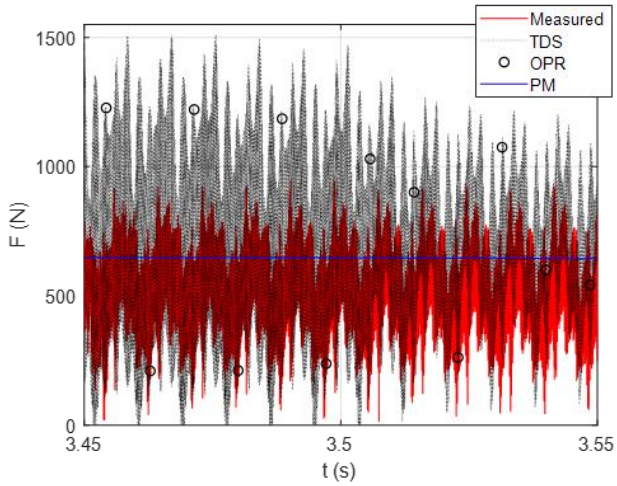

Figure 14. Resultant force for the ramp profile near center of toolpath. The axial depth is 12 mm and chatter is observed.

7. CONCLUSIONS

This paper combined time-domain milling simulation and feed rate scheduling software to predict dynamic cutting force components. The time-domain simulation inputs included the tool tip frequency response functions, cutting force model, and instantaneous radial depth of cut. The radial depth of cut profiles were obtained from the feed rate scheduling software Production Module provided by Third Wave Systems.

Two sets of machining trials were completed. First, constant radial depth of cut tests were completed to validate the force model and time-domain simulation force predictions against measurement. Both stable and unstable (chatter) milling conditions were observed with good agreement between time-domain simulation and measurement results. Comparisons to Production Module peak force predictions were also completed. The trends agreed for stable cutting conditions. Second, a ramp geometry tool path was selected with variable radial depth of cut. Comparisons between measurements and time-domain simulation were completed for both stable and unstable cutting conditions. The variable radial depth was again predicted by Production Module and was input to the time-domain simulation. Production Module peak force predictions trends agreed with measurement and simulation for stable cutting conditions. This effort demonstrates the value when including structural dynamics in cutting force predictions for machining optimization.

REFERENCES

Altintaş, Y. and Budak, E., 1995. Analytical prediction of stability lobes in milling. CIRP annals, 44(1), pp.357-362.

Altintas, Y. and Erkorkmaz, K., 2003. Feedrate optimization for spline interpolation in high speed machine tools. CIRP Annals, 52(1), pp.297-302.

Budak, E. and Tunc, L.T., 2010. Identification and modeling of process damping in turning and milling using a new approach. CIRP annals, 59(1), pp.403-408.

Dong, J., Ferreira, P.M. and Stori, J.A., 2007. Feed-rate optimization with jerk constraints for generating minimum-time trajectories. International Journal of Machine Tools and Manufacture, 47(12-13), pp.1941-1955.

Honeycutt, A. and Schmitz, T., 2016. A new metric for automated stability identification in time domain milling simulation. Journal of Manufacturing Science and Engineering, 138(7) pp.074501.

Honeycutt, A. and Schmitz, T., 2017. Milling stability interrogation by subharmonic sampling, Journal of Manufacturing Science and Engineering, 139(4), pp.041009.

Insperger, T., Gradišek, J., Kalveram, M., Stepan, G., Winert, K. and Govekar, E., 2006. Machine tool chatter and surface location error in milling processes. J. Manuf. Sci. Eng., 128(4), pp.913-920.

Lee, B.Y., Tarng, Y.S. and Ma, S.C., 1995. Modeling of the process damping force in chatter vibration. International Journal of Machine Tools and Manufacture, 35(7), pp.951-962.

Schmitz, T.L. and Mann, B.P., 2006. Closed-form solutions for surface location error in milling. International Journal of Machine Tools and Manufacture, 46(12-13), pp.1369-1377.

Schmitz, T. and Smith, K.S., 2009. Machining Dynamics: Frequency Response to Improved Productivity, Springer Science.

Tyler, C. and Schmitz, T., 2013. Analytical process damping stability prediction. Journal of Manufacturing Processes, 15, pp.69-76.

Yazar, Z., Koch, K.F., Merrick, T. and Altan, T., 1994. Feed rate optimization based on cutting force calculations in 3-axis milling of dies and molds with sculptured surfaces. International Journal of Machine Tools and Manufacture, 34(3), pp.365-377.